Parity-violating observables of two-nucleon systems in effective field theory

C.-P. Liu*

T-16, Theoretical Division, Los Alamos National Laboratory, Los Alamos, New Mexico 87545, USA

Theory Group, Kernfysisch Versneller Instituut, University of Groningen, Zernikelaan 25, NL-9747 AA Groningen, The Netherlands

(Received 28 September 2006; published 6 June 2007)

A newly-proposed parity-violating nucleon-nucleon interaction based on effective field theory is studied in this work. Using the hybrid effective field theory treatment, it is found that the parity-violating phenomena at low energy, where S-P transitions dominate, can be well specified by a set of six parameters. This includes five low-energy constants, which are equivalent to the Danilov parameters, and an additional parameter that characterizes the long-range one-pion exchange and is proportional to the parity-violating pion-nucleon coupling constant h_π^1. Selected observables in two-nucleon systems are analyzed, with their dependences on these parameters being determined by employing high-quality wave functions.

DOI: 10.1103/PhysRevC.75.065501 PACS number(s): 24.80.+y, 21.30.−x, 25.40.−h, 11.30.Er

I. INTRODUCTION

Study of the parity-violating (PV) nucleon-nucleon (NN) interaction, $V^{\rm PV}$, and its associated nuclear PV phenomena begins with the report by Tanner [1] shortly after parity violation was confirmed experimentally in 1957. The first clear evidence is found a decade after by observing a nonzero circular polarization in the γ-decay of ^{181}Ta [2]. Although quite a few PV observables have been measured later on in various nuclear systems, ranging from simple two-body scattering to heavy nuclear reaction, our current understanding of nuclear parity violation is still far from complete (see, e.g., Refs. [3–6] for reviews of this field). The major difficulty is twofold: not only these experiments require high precision to discern the much smaller PV signals, but also in theory, the nonperturbative character of the quark-gluon dynamics makes a "first-principle" formulation of $V^{\rm PV}$ as yet impossible. Despite the difficulties and that the underlying theory, the $SU(3)\otimes SU(2)\otimes U(1)$ gauge theory, is well-established, the study of $V^{\rm PV}$ is still valuable for two main reasons. First, it is the only viable venue to observe the neutral weak interaction between two quarks at low energy. Second, it supplies more information about the nucleon-nucleon dynamics in addition to existing scattering data.

The phenomenological development of $V^{\rm PV}$ proceeds in a similar fashion as what has been achieved in the parity-conserving (PC) NN interaction—starting out from pure phase-shift analyses, then parametrization in meson exchange models, and finally to rigorous effective field theory (EFT) formulation nowadays. It is first pointed out by Danilov [7–9] that, at low energy, $V^{\rm PV}$ can be characterized by five S-P scattering amplitudes: λ_s^{pp}, λ_s^{np}, and λ_s^{nn} for $^1S_0$-$^3P_0$ transitions, λ_t for $^3S_1$-$^1P_1$ transition, and ρ_t for $^3S_1$-$^3P_1$ transition. This idea is generalized by Desplanques and Missimer [10,11] to an effective version—through the Bethe-Goldstone equation—which applies to many-body systems. On the other hand, formulations of $V^{\rm PV}$ in terms of meson exchange models can be dated back to the seminal works by Blin-Stoyle [12,13] and Barton [14]. The specific form involving one π-, ρ-, and ω-exchanges, $V_{\rm OME}^{\rm PV}$, then becomes the standard in this field after Desplanques, Donoghue, and Holstein (DDH) give their prediction of the seven PV meson-nucleon coupling constants, h_m^i's (m denotes the type of meson and i the isospin), based on a quark model calculation [15].[1] As explained in Ref. [3], $V_{\rm OME}^{\rm PV}$ has a close connection to the S-P amplitude formulation, $V_{S\text{-}P}^{\rm PV}$, at low energy: The amplitude ρ_t contains a long-range one-pion-exchange contribution, and the other amplitudes, including the short-range part of ρ_t, are all related to the vector-meson exchanges.

Most of the existing PV observables have been analyzed in the one-meson-exchange (OME) framework. However, a consistent constraint of the PV coupling constants is not realized yet. There are several reasons. On the experimental side, many data have large errors so are not very constrictive; also, these observables in terms of h_m^i's are not independent enough to allow a simultaneous determination of these seven parameters. On the theoretical side, several precise data involve many-body systems; the reliabilities of these calculations are questionable. As one can see from, e.g., Refs. [4,16,17], a two-dimensional constraint on the particular linear combinations of the isoscalar and isovector couplings already shows some discrepancy. Besides these possibilities, one might also wonder if the analysis framework, i.e., $V_{\rm OME}^{\rm PV}$, could be the culprit.

To address the last question, Zhu *et al.* [18] recently reformulate $V^{\rm PV}$ in the EFT framework to the order of Q (Q is the momentum scale). This new framework comes with two incarnations: one with pions fully integrated out, $V_{\not\pi}^{\rm PV}$, and the other with dynamical pions, $V_{\rm EFT}^{\rm PV}$. The pionless version only contains the short-range (SR) interaction, $V_{1,\rm SR}^{\rm PV}$, and it is specified by ten low-energy constants (LECs) at the superficial level. It can be argued that at this order, only five LECs are truly independent and can be exactly mapped to

*cpliu@lanl.gov

[1] As the conventional nomenclature, the "DDH" potential, could be somewhat misleading, it is referred as the PV one-meson-exchange potential, $V_{\rm OME}^{\rm PV}$, in this work. We thank B. Desplanques for this clarification.

the five S-P amplitudes.[2] In the pionful version, dynamical pions generate two explicit terms: the leading-order, long-range (LR) interaction, $V^{\rm PV}_{-1,{\rm LR}}$, due to the one-pion exchange (OPE), and the sub-leading-order, medium-range (MR) interaction, $V^{\rm PV}_{1,{\rm MR}}$, due to the two-pion exchange (TPE). While the OPE part is also familiar in $V^{\rm PV}_{\rm OME}$, the TPE part has never been systematically treated before. By considering vertex corrections to the OPE term, the original formulation by Zhu *et al.* contains an extra next-to-next-to-leading-order interaction, $V^{\rm PV}_{1,{\rm LR}}$, whose operator structure is thought to be different from others already being specified. This term has recently been shown as redundant [19], so will be ignored in our discussion. Overall, in addition to the five LECs in the SR interaction, the pionful theory introduces, to $\mathcal{O}(Q)$, two more parameters: one with the interaction (h^1_π) and the other with the pion-exchange current ($\bar{c}_\pi$). An important point to note is that, although $V^{\rm PV}_{1,{\rm SR}}$ takes the same form in both $V^{\rm PV}_{\rm EFT}$ and $V^{\rm PV}_{\not\pi}$, the LECs in these two EFT frameworks have different meanings: all the pion physics is included in the LECs for the pionless version; but it is singled out in the pionful version.

With the advance of experimental techniques showing promise of PV measurements in few-body systems—where reliable theoretical calculations are available—an extensive search program to re-analyze PV observables is sketched in Ref. [18]. The proposed re-analysis makes use of the "hybrid" EFT framework, which combines the state-of-the-art wave functions (from phenomenological potential-model calculations) and the most general form of $V^{\rm PV}$(from EFT techniques).[3] The immediate goal is to find out whether a more consistent picture of nuclear parity violation can be reached among few-body systems. The long-term goal of including other precise measurements in many-body systems certainly relies on the previous success.

This paper takes the first step dealing with two-nucleon systems at low energy. The aim is to express the observables, both existing and potentially possible, in terms of the EFT parameters, and to serve as a part of the database which the complete search program calls for. The general formalism is introduced in Sec. II. The connection between $V^{\rm PV}$ (both $V^{\rm PV}_{\not\pi}$ and $V^{\rm PV}_{\rm EFT}$) and the S-P amplitudes is studied in Sec. III. The observables of two-nucleon systems are discussed subsequently in Sec. IV, and a summary follows in Sec. V.

II. FORMALISM

A fully consistent study of nuclear PV phenomena in the EFT framework requires treating PC and PV interactions order by order on the same footing. On the other hand, the "hybrid" approach, which combines the state-of-the-art wave functions from phenomenology and the general operator structure from EFT, is shown to have quite some success. In this work, we follow the latter approach as outlined in Ref. [18].

A. Parity-conserving potential and wave functions

In the hybrid EFT framework, the unperturbed scattering and deuteron (the binding energy $E_{\mathcal{D}} \cong 2.22$ MeV) wave functions, $|\psi\rangle^{(\pm)}$ and $|\psi\rangle_{\mathcal{D}}$, are obtained by solving the Lippmann-Schwinger and Schrödinger equations, respectively,

$$(H_0 + V^{\rm PC} \mp i\epsilon)|\psi\rangle^{(\pm)} = E|\psi\rangle^{(\pm)}, \tag{1}$$

$$(H_0 + V^{\rm PC})|\psi\rangle_{\mathcal{D}} = x - E_{\mathcal{D}}|\psi\rangle_{\mathcal{D}}, \tag{2}$$

with a chosen high-quality phenomenological potential as $V^{\rm PC}$. In this work, we use Argonne v_{18} (AV18) [20] model exclusively. The model dependence of PV observables on strong potentials has been extensively studied in Refs. [21,22]; for most cases, no strong deviation from AV18 is found.

Since the PV interaction is small, we treat it as a first-order perturbation. The PV scattering amplitude, $\widetilde{M}$, is obtained by the first-order distorted-wave Born approximation

$$\widetilde{M} = {}^{(-)}\langle\psi|V^{\rm PV}|\psi\rangle^{(+)}. \tag{3}$$

The parity admixtures of the scattering and deuteron states, $|\widetilde{\psi}\rangle^{(\pm)}$ and $|\widetilde{\psi}\rangle_{\mathcal{D}}$, are obtained by solving the inhomogeneous differential equations

$$(E - H_0 - V^{\rm PC})|\widetilde{\psi}\rangle^{(\pm)} = V^{\rm PV}|\psi\rangle^{(\pm)}, \tag{4}$$

$$(E_{\mathcal{D}} + H_0 + V^{\rm PC})|\widetilde{\psi}\rangle_{\mathcal{D}} = -V^{\rm PV}|\psi\rangle_{\mathcal{D}}, \tag{5}$$

respectively, where the product of the PV potential and the unperturbed wave function serves as the source term. We refer more technical details regarding the partial wave expansion, phase shifts, and numerical procedures to Refs. [21–23], but only mention a subtle point about the phase convention: We adopt, exclusively, the Condon-Shortley phase convention; it is different from the Biedenharn-Rose phase convention which contains an additional phase i^L for the partial wave of orbital angular momentum L.

B. Parity-violating interaction in pionless EFT

In the pionless EFT, the PV interaction is entirely short-ranged and takes the following form in the coordinate space [18]:

$$\begin{aligned} V^{\rm PV}_{\not\pi}(\boldsymbol{r}) &= V^{\rm PV}_{1,{\rm SR}}(\boldsymbol{r}) \\ &= \frac{2}{\Lambda_\chi^3}\{[C_1 + (C_2 + C_4)\tau^z_+ + C_3\tau_\cdot \\ &\quad + C_5\tau^{zz}]\boldsymbol{\sigma}_- \cdot \boldsymbol{y}_{m+}(\boldsymbol{r}) \\ &\quad + [\tilde{C}_1 + (\tilde{C}_2 + \tilde{C}_4)\tau^z_+ + \tilde{C}_3\tau_\cdot \\ &\quad + \tilde{C}_5\tau^{zz}]\boldsymbol{\sigma}_\times \cdot \boldsymbol{y}_{m-}(\boldsymbol{r}) \\ &\quad + (C_2 - C_4)\tau^z_-\boldsymbol{\sigma}_+ \cdot \boldsymbol{y}_{m+}(\boldsymbol{r}) \\ &\quad + \tilde{C}_6\tau^z_\times\boldsymbol{\sigma}_+ \cdot \boldsymbol{y}_{m-}(\boldsymbol{r})\}, \end{aligned} \tag{6}$$

where Λ_χ is the scale of chiral symmetry breaking and related to the pion decay constant F_π by $\Lambda_\chi = 4\pi F_\pi \approx 1.161$ GeV;

[2] One simple way to argue this is the following. At short distances, the radial function of the partial wave with orbital angular momentum l scales like r^l. Therefore, to the order of Q—with Q acting like d/dr—only five S-P mixings can be induced by the EFT contact interaction (higher partial wave mixings need higher orders of Q).

[3] This is a temporary step until an EFT strong potential is developed to the required precision.

$\tau_\cdot \equiv \boldsymbol{\tau}_1 \cdot \boldsymbol{\tau}_2$, $\tau^z_\pm \equiv (\tau^z_1 \pm \tau^z_2)/2$, $\tau^z_\times \equiv i(\boldsymbol{\tau}_1 \times \boldsymbol{\tau}_2)^z/2$, and $\tau^{zz} \equiv (3\tau^z_1\tau^z_2 - \boldsymbol{\tau}_1 \cdot \boldsymbol{\tau}_2)/(2\sqrt{6})$ are the isospin operators;[4] $\boldsymbol{\sigma}_\pm \equiv \boldsymbol{\sigma}_1 \pm \boldsymbol{\sigma}_2$ and $\boldsymbol{\sigma}_\times \equiv i\boldsymbol{\sigma}_1 \times \boldsymbol{\sigma}_2$ are the spin operators. The spatial operator $\boldsymbol{y}_{m-(+)}(\boldsymbol{r})$ is defined as the (anti-) commutator of $-i\nabla$ with the mass^2-weighted Yukawa function $f_m(r)$

$$\boldsymbol{y}_{m\pm}(\boldsymbol{r}) = [-i\nabla,\, f_m(r)]_\pm \equiv \left[-i\nabla,\, m^2\frac{\mathrm{e}^{-mr}}{4\pi r}\right]_\pm . \tag{7}$$

When $m \to \infty$, $f_m(r) \to \delta(r)/r^2$; the potential thus takes a four-fermion contact form as expected.

While using a Yukawa functional form for $f_m(r)$ leads to a similar spatial behavior as the conventional $V^{\rm PV}_{\rm OME}$, other choices—as long as they are realized in the context of EFT—are also possible. For instance, taking into account the monopole form factors at both the strong and weak vertices with a cutoff Λ_m, one obtains a modified Yukawa function

$$\bar{f}_m(r) = \frac{m^2}{4\pi r}\left\{\mathrm{e}^{-mr} - \mathrm{e}^{-\Lambda_m r}\left[1 + \frac{1}{2}\left(1 - \frac{m^2}{\Lambda_m^2}\right)\Lambda_m r\right]\right\}. \tag{8}$$

At the $\Lambda_m \to \infty$ limit, $\bar{f}_m(r)$ recovers the "bare" Yukawa form $f_m(r)$. We note that in Refs. [21,22], a recent and extensive OME analyses of two-body nuclear PV, the authors adopt $\bar{f}_m(r)$ instead of the conventional choice $f_m(r)$.

At this point, we emphasize that the Yukawa function serves as a regulator for the strict contact interaction (as a delta function). Therefore, the Yukawa mass m should be realized as a cutoff scale for the short range: for pionless theory, $m \gtrsim m_\pi$; for pionful theory, $m \gtrsim m_\rho, \Lambda_\chi$—with some arbitrariness. While all the LECs C's and $\tilde{C}$'s defined here should bear this regulator dependence, the physical results should not, as will be illustrated in later sections.

As $\tilde{C}_2$ and $\tilde{C}_4$ appear as a linear combination $\tilde{C}_2 + \tilde{C}_4$ in Eq. (6), $V^{\rm PV}_{1,\rm SR}$ contains $11 - 1 = 10$ LECs at the superficial level. After resolving the isospin and spin matrix elements of all allowed two-nucleon states, the PV observables depend on the following ten linear combinations of C's and $\tilde{C}$'s:

(i) pp: $D^{pp}_v = C_1 + C_3 + C_2 + C_4 + C_5/\sqrt{6}$ and $\tilde{D}^{pp}_v = \tilde{C}_1 + \tilde{C}_3 + [\tilde{C}_2 + \tilde{C}_4] + \tilde{C}_5/\sqrt{6}$,
(ii) nn: $D^{nn}_v = C_1 + C_3 - C_2 - C_4 + C_5/\sqrt{6}$ and $\tilde{D}^{nn}_v = \tilde{C}_1 + \tilde{C}_3 - [\tilde{C}_2 + \tilde{C}_4] + \tilde{C}_5/\sqrt{6}$,
(iii) $np|_{T_i=T_f=1}$: $D^{np}_v = C_1 + C_3 - 2C_5/\sqrt{6}$ and $\tilde{D}^{np}_v = \tilde{C}_1 + \tilde{C}_3 - 2\tilde{C}_5/\sqrt{6}$,
(iv) $np|_{T_i=T_f=0}$: $D_u = C_1 - 3C_3$ and $\tilde{D}_u = \tilde{C}_1 - 3\tilde{C}_3$,
(v) $np|_{T_i\neq T_f}$: $D_w = C_2 - C_4$ and $\tilde{D}_w = \tilde{C}_6$.

[4]The operators τ^{zz} and $\tau^z_\times$ we adopt are different from Ref. [18]. Therefore, the LECs C_5, $\tilde{C}_5$, and $\tilde{C}_6$ in our definition are greater than their counterparts in Ref. [18] by factors of $-2\sqrt{6}$, $-2\sqrt{6}$, and 2, respectively. Also note that the notation of C_6 in Ref. [18] is changed into $\tilde{C}_6$ in this paper, because it is associated with a $\boldsymbol{y}_{m-}$ type operator like other $\tilde{C}$'s.

C. Parity-violating interaction in pionful EFT

When pions are treated explicitly, the EFT PV interaction, as formulated in Ref. [18], contains three parts[5]

$$V^{\rm PV}_{\rm EFT}(\boldsymbol{r}) = V^{\rm PV}_{-1,\rm LR}(\boldsymbol{r}) + V^{\rm PV}_{1,\rm MR}(\boldsymbol{r}) + V^{\rm PV}_{1,\rm SR}(\boldsymbol{r}). \tag{9}$$

For the SR interaction, even though it takes the same operator structure as in the pionless theory, one has to adopt a bigger Yukawa mass. A very useful choice is $m \sim m_\rho, m_\omega$. In this case, $V^{\rm PV}_{1,\rm SR}$ is tantamount to the ρ- and ω-sectors of $V^{\rm PV}_{\rm OME}$ if one assumes the following relations between $\tilde{C}$'s and C's:

$$\frac{\tilde{C}_1}{C_1} = \frac{\tilde{C}_2}{C_2} = 1 + \chi_\omega, \tag{10a}$$

$$\frac{\tilde{C}_3}{C_3} = \frac{\tilde{C}_4}{C_4} = \frac{\tilde{C}_5}{C_5} = 1 + \chi_\rho, \tag{10b}$$

where χ_ω and χ_ρ are the isoscalar and isovector strong tensor couplings, respectively. The remaining $11 - 5 = 6$ LECs then have a one-to-one mapping to the PV heavy-meson-nucleon coupling constants as

$$(C_1, C_2) \to -\frac{g_\omega}{2}\left(h^0_\omega, h^1_\omega\right)\frac{\Lambda^3_\chi}{m_N m^2_\omega}, \tag{11a}$$

$$(C_3, C_4, C_5, \tilde{C}_6) \to -\frac{g_\rho}{2}\left(h^0_\rho, h^1_\rho, h^2_\rho, h^{1'}_\rho\right)\frac{\Lambda^3_\chi}{m_N m^2_\rho}, \tag{11b}$$

where g_x denotes the strong x-meson-nucleon coupling constant. Note that in analyses based on $V^{\rm PV}_{\rm OME}$, the $h^{1'}_\rho$ part is usually ignored because it has the same operator structure as the LR OPE interaction, i.e., the h^1_π part, but a very small predicted value for $h^{1'}_\rho$.

The leading term $V^{\rm PV}_{-1,\rm LR}$ is the familiar PV OPE potential

$$V^{\rm PV}_{-1,\rm LR}(\boldsymbol{r}) = \frac{2}{\Lambda^3_\chi}\tilde{C}^\pi_6 \tau^z_\times \boldsymbol{\sigma}_+ \cdot \boldsymbol{y}_{\pi-}(\boldsymbol{r}), \tag{12}$$

with

$$\tilde{C}^\pi_6 = \frac{h^1_\pi g_A}{2\sqrt{2}}\frac{\Lambda^3_\chi}{F_\pi m^2_\pi} = \frac{h^1_\pi g_\pi}{2\sqrt{2}}\frac{\Lambda^3_\chi}{m_N m^2_\pi}, \tag{13}$$

where $g_A = 1.27$ is the nucleon axial vector coupling constant and $m_\pi = 139.57$ MeV; and the second equality follows from the Goldberger-Trieman relation.

The subleading MR interaction is due to TPE and has the form[6]

$$V^{\rm PV}_{1,\rm MR}(\boldsymbol{r}) = \frac{2}{\Lambda^3_\chi}\left\{\tilde{C}^{2\pi}_2 \tau^z_+ \boldsymbol{\sigma}_\times \cdot \boldsymbol{y}^L_{2\pi-}(\boldsymbol{r}) + \tilde{C}^{2\pi}_6 \tau^z_\times \boldsymbol{\sigma}_+ \cdot \left[\left(1 - 1/\left(3g^2_A\right)\right)\boldsymbol{y}^L_{2\pi-}(\boldsymbol{r}) - 1/3\,\boldsymbol{y}^H_{2\pi-}(\boldsymbol{r})\right]\right\}, \tag{14}$$

[5]As mentioned in the Introduction, we ignore the higher-order LR term $V^{\rm PV}_{1,\rm LR}$ in Ref. [18], since it is shown to be redundant [19].

[6]Some mistakes in Eq. (121) of Ref. [18] have been fixed in order to produce Eqs. (15) and (16); see also Ref. [24]. We thank B. Desplanques and Zhu *et al.* for pointing this out.

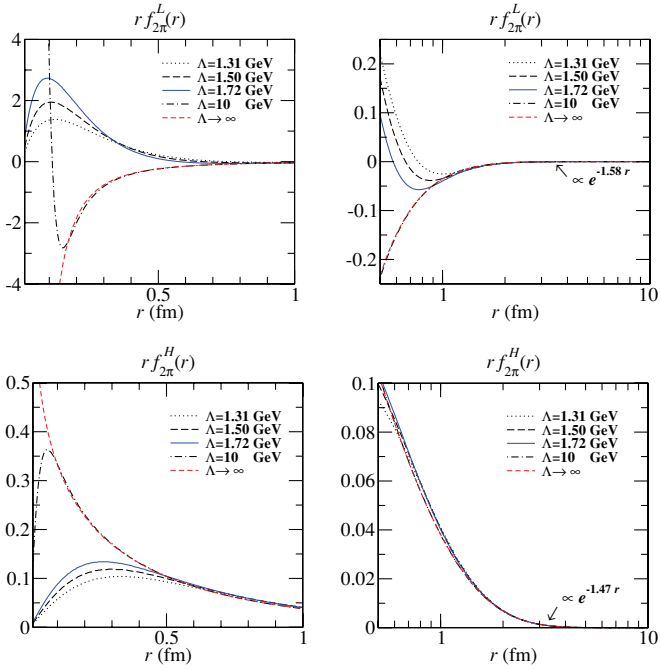

FIG. 1. (Color online) The r-weighted Yukawa-like radial functions $rf^L_{2\pi}(r)$ and $rf^H_{2\pi}(r)$ in the two-pion-exchange potential.

with

$$\tilde{C}^{2\pi}_2 = -4\sqrt{2}\pi g_A^3 h^1_\pi, \tag{15}$$

$$\tilde{C}^{2\pi}_6 = 3\sqrt{2}\pi g_A^3 h^1_\pi. \tag{16}$$

The Yukawa-like radial functions $f^L_{2\pi}(r)$ and $f^H_{2\pi}(r)$, for generating $\boldsymbol{y}^L_{2\pi} - (\boldsymbol{r})$ and $\boldsymbol{y}^H_{2\pi} - (\boldsymbol{r})$ via Eq. (7), are obtained from the Fourier transforms of

$$L(q) = \frac{\sqrt{4m_\pi^2 + \boldsymbol{q}^2}}{|\boldsymbol{q}|} \ln\left(\frac{\sqrt{4m_\pi^2 + \boldsymbol{q}^2} + |\boldsymbol{q}|}{2m_\pi}\right), \tag{17}$$

$$H(q) = \frac{4m_\pi^2}{4m_\pi^2 + \boldsymbol{q}^2} L(q), \tag{18}$$

respectively. In Fig. 1, the plots of $rf^L_{2\pi}(r)$ and $rf^H_{2\pi}(r)$ are shown with several dipole cutoff factors $(\Lambda^2 - 4m_\pi^2)^2/(\Lambda^2 + q^2)^2$—including the bare case, i.e., $\Lambda \to \infty$—introduced in the Fourier transforms. As one clearly sees, the short distance behaviors are quite cutoff-sensitive, especially for $f^L_{2\pi}(r)$ since $L(q)$ diverges logarithmically as $\ln q/m_\pi$. On the other hand, the long-range tails, roughly decrease like $e^{-1.58r}$ and $e^{-1.47r}$, track well with $e^{-2m_\pi r} = e^{-1.41r}$.

The way we define $\tilde{C}^\pi_6, \tilde{C}^{2\pi}_2$, and $\tilde{C}^{2\pi}_6$ is handy for the bookkeeping purpose; this gives $V^{\rm PV}_{-1,\rm LR}$ and $V^{\rm PV}_{1,\rm MR}$ the same formal structure as the corresponding parts—as hinted by the subscripts—in $V^{\rm PV}_{1,\rm SR}$ (also, all the Yukawa functions $f_m(r)$, $f_\pi(r)$, $f^L_{2\pi}(r)$, and $f^H_{2\pi}(r)$ have the same limit when $m, m_\pi \to \infty$). However, this does not imply these pion PV constants are comparable in magnitude with LECs C's and $\widetilde{C}$'s. Comparing Eqs. (13), (15), and (16), one sees $\tilde{C}^{2\pi}_{2,6}$ smaller than $\tilde{C}^\pi_6$ roughly by an order of magnitude. By Eqs. (11a) and (11b) and assuming all the π-, ρ-, and ω-coupling constants approximately the same, one estimates C's smaller than $\tilde{C}^\pi_6$ roughly by a factor of $m_\rho^2/m_\pi^2 \sim 30$; for $\widetilde{C}$'s, due to the tensor couplings, Eqs. (10a) and (10b), the suppression can be less. If the above assumptions are not too far off, we can roughly conclude that $\tilde{C}^{2\pi}_{2,6}$ and the LECs, C's and $\widetilde{C}$'s, are of the same order, and all of them smaller than $\tilde{C}^\pi_6$ by an order of magnitude. This observation is consistent with the power counting scheme that both the MR and SR terms are of the same higher order than the OPE one. But, more definitive answer should still be sought from experiments.

We also emphasize that the MR term $V^{\rm PV}_{1,\rm MR}$, as expressed in Eq. (14), is not the full PV TPE potential. According to Ref. [18], it only contains the non-analytic part of the TPE, and all the analytic terms are effectively included in the short-range interaction. In this sense, $V^{\rm PV}_{\rm EFT}$ in fact depends on the chosen regularization scheme, in addition to the cutoff dependence already mentioned above.

TABLE I. Sets of strong parameters used for OME mapping.

	g_π	g_ρ	g_ω	κ_ρ	κ_ω
DDH-best [3]	13.45	2.79	8.37	3.70	−0.12
DDH-adj. [22]	13.22	3.25	15.85	6.10	0.0

D. Setup and parameters

In the following sections, various PV observables in two-nucleon systems will be analyzed by $V^{\rm PV}_{\rm EFT}$. The Yukawa mass parameter in $V^{\rm PV}_{1,\rm SR}$ is fixed to the ρ meson mass, $m = m_\rho = 771.1$ MeV, since this has an easy connection to the meson-exchange picture. For the convenience of presentation, these calculations will be referred as the "bare" calculations, because all Yukawa functions in $V^{\rm PV}_{\rm EFT}$ are not modified by any form factor. The results will be checked against existing calculations in the $V^{\rm PV}_{\rm OME}$ framework. This is done by applying the relations Eqs. (10a), (10b), (11b), (11a), and (13) to $V^{\rm PV}_{\rm EFT}$ and ignoring all the TPE contribution; from now on, we call this procedure OME-mapping (OME-m). For numerical estimates, the strong parameters are taken from Ref. [3] and the weak ones are set to be the "best-guess" values of DDH [15]. This set is labeled as "DDH-best" in Tables I and II.

In order to compare with Refs. [21,22], as pointed out previously, one has to use the monopole-modified Yukawa functions instead. For this matter, we perform a parallel set of calculations using $\bar{f}_m(r)$ with the cutoff parameters chosen to be $\Lambda_{\rm SR} = 1.31$GeV for the SR interaction and $\Lambda_{\rm LR} = \Lambda_{\rm MR} =$

TABLE II. Sets of weak parameters used for OME mapping (in units of 10^{-7}). Note that for pp systems, $h^0_\rho + h^1_\rho + h^2_\rho/\sqrt{6} = -22.3$, instead of -24.8 as shown in this table, will be used [21].

	h^1_π	h^0_ρ	h^1_ρ	h^2_ρ	h^0_ω	h^1_ω	$h^{1'}_\rho$
DDH-best [15]	4.56	−11.4	−0.19	−9.50	−1.90	−1.14	0.00
DDH-adj. [21,22]	4.56	−16.4	−2.77	−13.7	+3.23	+1.94	0.00

1.72 GeV for the LR and MR ones; they correspond to Λ_ρ and Λ_π in Ref. [22], respectively. These calculations will be referred as the "mod" calculations. For numerical results in this set of calculations, the strong parameters are taken from the Bonn model [25] and the weak ones are the fitted results of Refs. [21,22]. This set is labeled as "DDH-adj." in Tables I and II.

In addition, we also perform calculations in the pionless framework, $V_{\not\pi}^{\rm PV}$, with the Yukawa mass scale set to be $m = m_\pi$. In this case, calculations using bare and modified Yukawa functions do not differ a lot, so we only quote the bare one. This set is labeled as "π-less".

III. S-P AMPLITUDES AND DANILOV PARAMETERS

A PV potential with 11 (10 LECs plus h_π^1) undetermined parameters certainly poses a formidable challenge—how can we gather sufficient data and do reliable theoretical analyses of them? A substantial reduction of the LECs is proposed in Ref. [18] by building the connection to the S-P amplitude analysis, which is pioneered by Danilov [7–9], and extended by Desplanques and Missimer later on [10,11,26]. The main idea of this reduction goes like the following.

For low-energy PV phenomena in which only the S-P mixings contribute substantially, the observables can be expressed by five independent PV scattering amplitudes: $v_{pp,nn,np}(^1S_0 \to {}^3P_0)$, $u(^3S_1 \to {}^1P_1)$, and $w(^3S_1 \to {}^3P_1)$. From the last section, we know each amplitude due to $V_{1,\rm SR}^{\rm PV}$ is a linear combination of the corresponding D and $\widetilde{D}$ with the coefficients being determined by the matrix elements of $\boldsymbol{y}_{m+}$ and $\boldsymbol{y}_{m-}$, respectively. An important observation comes from that the matrix elements $\langle \boldsymbol{y}_{m+}\rangle$ and $\langle \boldsymbol{y}_{m-}\rangle$ are equal in the zero-range approximation (ZRA). This causes D and $\widetilde{D}$ always appear in a $(D+\widetilde{D})$ combination which works actually like one energy-independent LEC. Therefore, the number of LECs can be reduced to five which corresponds to the number of independent S-P amplitudes and reflects the actual EFT counting. In order to implement this idea in the hybrid EFT treatment properly, we try to address the following issues:

(i) The 10-to-5 reduction can still work as long as the matrix elements of $\boldsymbol{y}_{m+}$ and $\boldsymbol{y}_{m-}$ have (almost) the same energy dependence, i.e., the condition

$$\frac{\langle \boldsymbol{y}_{m+}\rangle}{\langle \boldsymbol{y}_{m-}\rangle} \equiv R(E;m) \cong R(m), \tag{19}$$

is satisfied. Note that this ratio depends on the Yukawa mass scale (and also Λ_m if a modified Yukawa function is used). Even though it is not a physical quantity, it gives a rough estimate how this reduction in the hybrid EFT scheme would work with a chosen m.

(ii) When higher partial waves become important, the S-P analyses are no longer valid. We try to estimate the energies when D-P transitions become non-negligible.

(iii) The pionless EFT works for $Q \lesssim m_\pi$, which corresponds to $E_{\rm lab} \lesssim 10$ MeV. We also examine the 10-to-5 reduction in this framework.

(iv) At the end of this section, we determine the zero-energy S-P amplitudes, the so-called Danilov parameters, in terms of the PV parameters. They will be the actual physical parameters used to express the PV observables in the next section.

According to the definitions by Desplanques and Missimer [10], the S-P amplitudes are calculated by the following formulas:

$$\begin{aligned} v &= \frac{m_N}{ip}\frac{\langle {}^3P_0|V_{\rm EFT}^{\rm PV}|{}^1S_0\rangle}{\langle {}^3P_0|\boldsymbol{\sigma}_-\cdot\hat{r}|{}^1S_0\rangle}\frac{e^{\eta\pi}}{|\Gamma(1+i\eta)||\Gamma(2+i\eta)|} \\ &= v^-\tilde{D}_v + v^+ D_v + v^{2\pi}\tilde{C}_2^{2\pi}, \end{aligned} \tag{20a}$$

$$\begin{aligned} u &= \frac{-m_N}{ip}\frac{\langle {}^1P_1|V_{\rm EFT}^{\rm PV}|{}^3S_1\rangle}{\langle {}^1P_1|\boldsymbol{\sigma}_-\cdot\hat{r}|{}^3S_1\rangle} \\ &= u^-\tilde{D}_u + u^+ D_u, \end{aligned} \tag{20b}$$

$$\begin{aligned} w &= \frac{-m_N}{ip}\frac{\langle {}^3P_1|V_{\rm EFT}^{\rm PV}|{}^3S_1\rangle}{\langle {}^3P_1|\boldsymbol{\sigma}_+\cdot\hat{r}|{}^3S_1\rangle} \\ &= w^-\tilde{D}_w + w^+ D_w + w^\pi\tilde{C}_6^\pi + w^{2\pi}\tilde{C}_6^{2\pi}, \end{aligned} \tag{20c}$$

where all the amplitudes are functions of energy, p is the two-nucleon relative momentum, and the factors are chosen to reproduce the normalization and limiting behaviors of Refs. [5,10]. Note that for the v amplitude, an extra factor, which is 1 when the Sommerfeld number $\eta = 0$, is introduced in order to completely subtract the Coulomb effect for pp scattering at threshold.

Since the total cross section is proportional to the imaginary part of the forward scattering amplitude, we concentrate on Im$[v, u, w]$, and start with the cases of pionful theory, $m = m_\rho$.

The top panels of Fig. 2 show the energy dependences of the x^--type S-P amplitudes ($x \in v_{pp,nn,np}, u, w$), proportional to $\langle \boldsymbol{y}_{m-}\rangle$, up to $E_{\rm lab} = 100$ MeV. Because the form factors suppress the short-distance contributions, the results from the "mod" calculations are consistently smaller than the "bare" ones. On the other hand, their energy dependences are almost the same, which implies the cutoff effect can be simply simulated by an overall factor. Another noticeable feature is the plots of v_{pp}, v_{nn}, and v_{np} overlap, and the tiny difference is mostly due to the small charge-dependent interaction built in AV18.

The bottom panels of Fig. 2 show the percentage deviations of x^+/x^- from their zero-energy values $x^+(0)/x^-(0)$, i.e.,

$$\Delta x^+/x^- \equiv \frac{x^+/x^- - x^+(0)/x^-(0)}{x^+(0)/x^-(0)}. \tag{21}$$

In case the energy dependences of x^+ and x^- keep the same, $\Delta x^+/x^-$ remains zero. Therefore, this quantity is a measure of the departure from the perfect scaling, Eq. (19), which a strict 10-to-5 reduction scheme requires. As these plots show, the deviations all grow with energy in the positive direction. For the v and w amplitudes, the scaling actually works very well—though not perfect—up to $E_{\rm lab} = 100$ MeV where the deviations are still less than 10% for the "bare" case. For the u amplitude, however, the 10% tolerance for scaling deviation

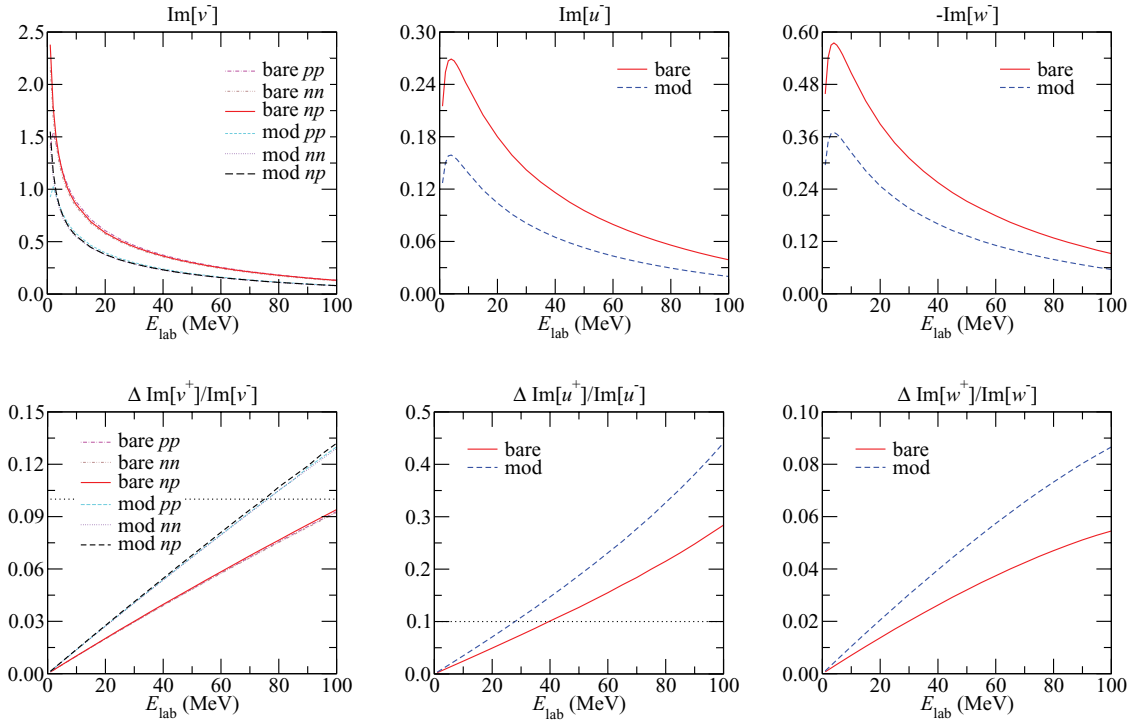

FIG. 2. (Color online) Top panels: the energy dependences of the x^--type S-P amplitudes. Bottom panels: the percentage deviations of x^+/x^- from their zero-energy values $x^+(0)/x^-(0)$, where the dotted lines mark the 10% level.

can only allow $E_{\rm lab}$ go as high as 40 MeV.[7] It might come as a surprise why the u and w amplitudes have such different behaviors, since both involve the same ${}^3S_1$ wave and the ${}^1P_1$ wave (for u) does not differ from the ${}^3P_1$ one (for w) dramatically. The answer is due to the tensor force, by which a true distorted ${}^3S_1$-wave acquires some D-wave component. From the ratios

$$\langle {}^1P_1|\boldsymbol{\sigma}_-\cdot\hat{r}|{}^3S_1, L=2\rangle/\langle {}^1P_1|\boldsymbol{\sigma}_-\cdot\hat{r}|{}^3S_1, L=0\rangle = -\sqrt{2}, \tag{22}$$

$$\langle {}^3P_1|\boldsymbol{\sigma}_+\cdot\hat{r}|{}^3S_1, L=2\rangle/\langle {}^3P_1|\boldsymbol{\sigma}_+\cdot\hat{r}|{}^3S_1, L=0\rangle = 1/\sqrt{2}, \tag{23}$$

one learns that the D-wave component is more enhanced in the u than the w amplitude, and this is the main cause of the difference. A mock calculation by pretending the ratio in Eq. (22) to be $1/\sqrt{2}$ as in Eq. (23) verifies that the scaling of u^+/u^- would then be similar to w^+/w^-. The "mod" calculations generally show larger deviations, so the ranges within which the scaling works have to be reduced. This can be understood from that the difference of $\boldsymbol{y}_{m+}$ and $\boldsymbol{y}_{m-}$ is a term involving the gradient on the wave function. As the form factor suppresses the short-range contribution, the longer-range part of the wave function which has a larger gradient thus gets a bigger weight; this leads to an enhancement of the deviation.

The importance of the D-P transitions is illustrated in Fig. 3, where their ratios to the S-P counterparts are shown for $x^{-,\pi,2\pi}$-type amplitudes. For the v-type amplitudes, which involve the SR and MR interactions, the D-P transitions appear to be non-negligible when energy reaches $E_{\rm lab} \sim 70$–90 MeV. For the u-type amplitude, which purely comes from the SR interaction, the D-P transition starts to kick in at a smaller energy $E_{\rm lab} \sim 30$–50 MeV. The more complex case is the w-type amplitude, where the LR, MR, and SR interactions all contribute. As one expects the LR interaction plays the most important role, the D-P transitions (could be ${}^3D_1$-${}^3P_1$ or ${}^3D_2$-${}^3P_2$) can become important when energy reaches $E_{\rm lab} \sim 20$–40 MeV. The reason that the importance of ${}^3D_2$-${}^3P_2$ mixing rapidly increases with energy is mainly because the first node of ${}^3D_2$ wave occurs at a relatively large distance $r \gtrsim 5$ fm, while the first node of ${}^3S_1$-${}^3D_1$ wave occurs at $r \sim 2$–4 fm, which leads to cancellation between short- and large-distance contributions. As these D-P amplitudes have quite different energy dependences compared to the S-P ones, the 10-to-5 reduction should also be subject to this prerequisite of S-P dominance, which is more stringent.

In Fig. 4, whether the OPE and TPE contributions can be effectively included in the SR potential is studied by examining the scaling behaviors of the LR and MR amplitudes $x^{\pi,2\pi}$ with respect to x^-. As one can see, all the deviations increase with energy in the negative direction. In the "bare" calculations, the MR amplitudes scale very well with the SR

[7]This 10% level is mainly set to match the precision which future PV experiments aim at. One can certainly relax this very conservative estimate to a 20–30% level, which corresponds to the typical size of chiral expansion parameters.

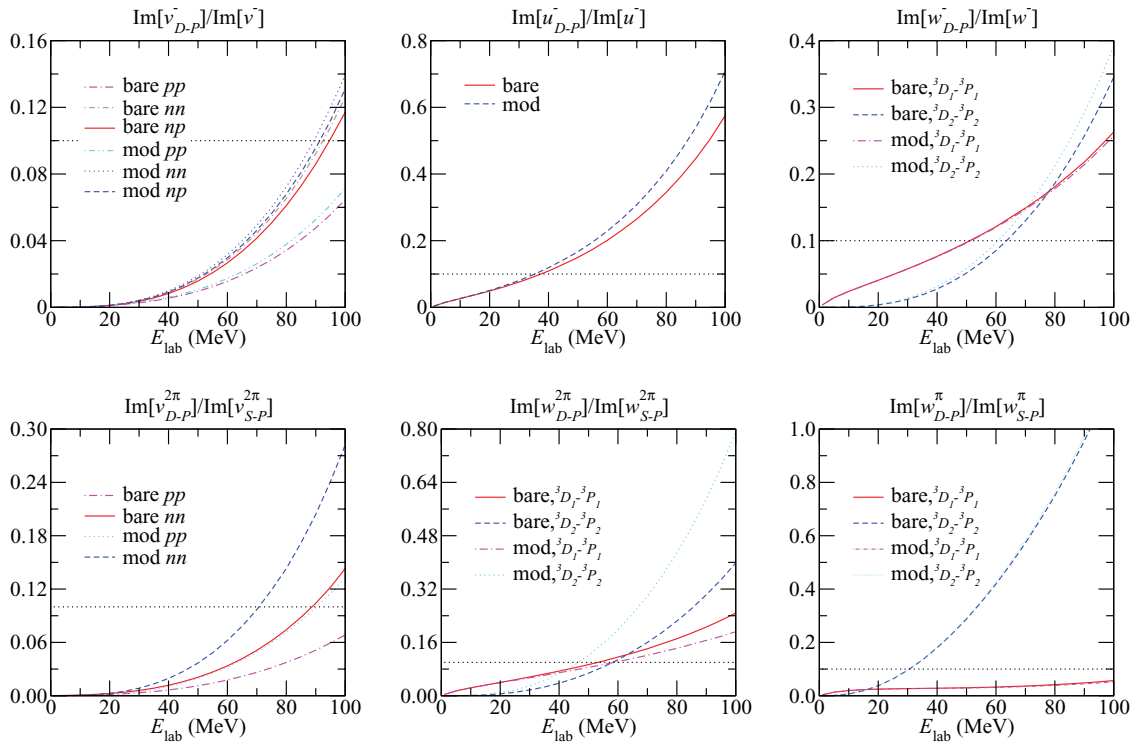

FIG. 3. (Color online) The ratios of the D-P to S-P transition amplitudes of $x^{-,\pi,2\pi}$-types as functions of energy, where the dotted lines mark the 10% level.

one. Allowing a 10% deviation, the scaling works as $E_{\rm lab}$ reaches up to more than 100 MeV for the v amplitudes and 60 MeV for the w one; both limits are less constrictive than the S-P-dominant requirement. On the other hand, the scaling works quite poorly—only up to $E_{\rm lab} = 20$ MeV—in the "mod" calculations—this can be easily seen from Fig. 1, where the modified two-pion Yukawa-like functions differ substantially from the bare ones at short distances—but still consistent with the S-P-dominant requirement.

The most noteworthy information in Fig. 4 comes from the observation that it is almost impossible for the OPE amplitude to scale with the SR one (with $m = m_\rho$), unless within a very restricted energy range, e.g., near threshold. From threshold to 20 MeV, in which the S-P dominance holds for the w amplitude, the scaling deviation increases to 40%. Thus, this reconfirms the old wisdom that it takes two parameters—one for the SR and the other for the LR term—to characterize the physics of the ${}^3S_1$-${}^3P_1$ transition [3,10].

We also note at this point that when pions have to be kept as explicit degrees of freedom, it is not required that the MR amplitude (from TPE) has the same energy dependence as the SR amplitudes: the scaling between MR and SR amplitudes does not result in any reduction of required parameters. In fact, as the MR and SR interactions have different ranges—the former being $\sim 1/(2m_\pi)$ and the latter being $\sim 1/\Lambda_\chi$—one would expect they should have different energy dependences

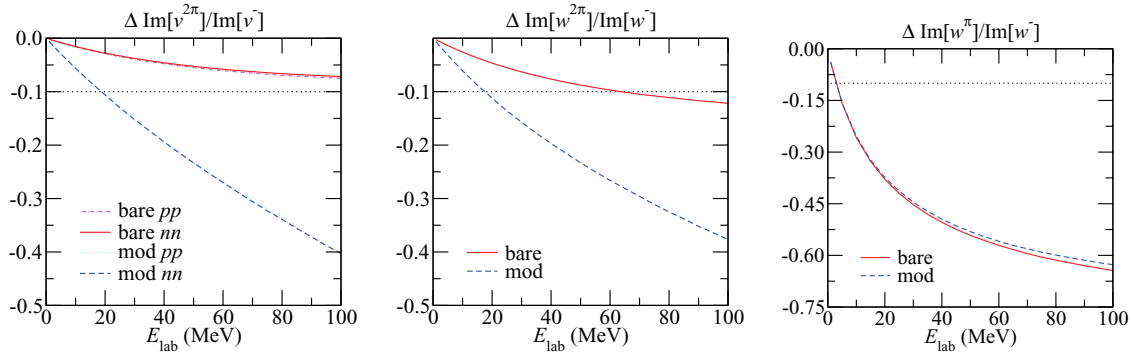

FIG. 4. (Color online) The percentage deviations of $x^{\pi,2\pi}/x^{-}$ from their zero-energy values $x^{\pi,2\pi}(0)/x^{-}(0)$, where the dotted lines mark the 10% level.

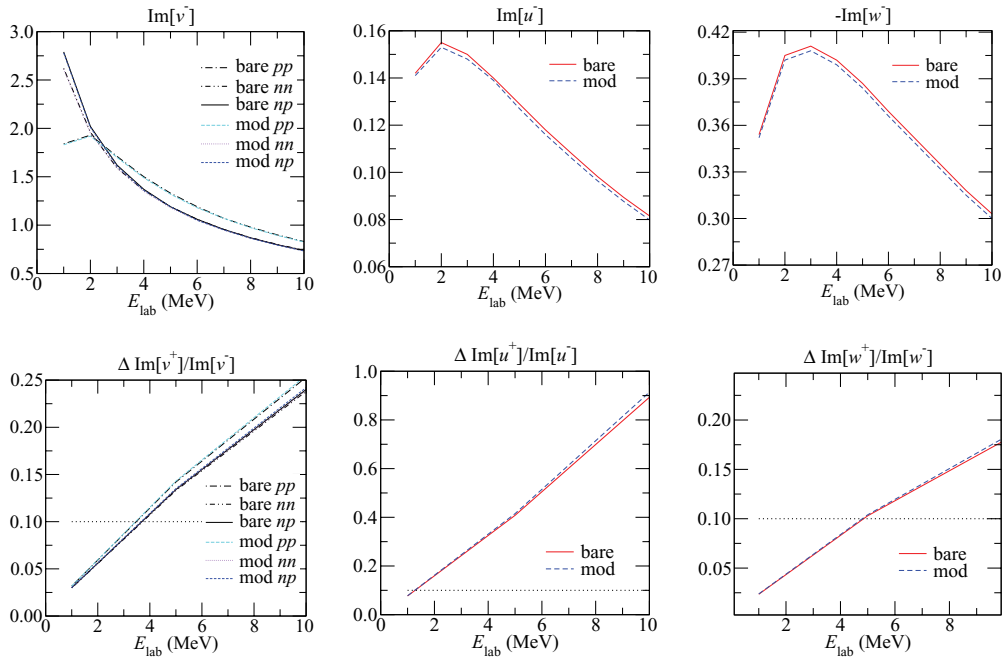

FIG. 5. (Color online) The similar analysis as Fig. 2 for the x^- and x^+ amplitudes with the Yukawa mass parameter in $V^{\rm PV}_{+1,\rm SR}$ chosen to be $m = m_\pi$. The dotted lines mark the 10% level.

over a broad energy range. However, in the considered range of S-P dominance, as these two amplitudes (with the chosen cutoffs) do not differ too much in energy dependence, we will group them together for the following discussions and only single out the OPE part.

The similar analysis as Fig. 2 for the pionless framework with $m = m_\pi$ is presented in Fig. 5; and the plots only extend to $E_{\rm lab} = 10$ MeV—beyond which one would not expect a pionless theory work properly. As the range of the interaction $\sim 1/m_\pi$ is somewhat longer than the one in pionful calculations, the results are rather insensitive to the Yukawa cutoff Λ_m: one can see that the "bare" and "mod" plots hardly make much difference. The scaling of $\langle \boldsymbol{y}_{m+} \rangle$ and $\langle \boldsymbol{y}_{m-} \rangle$ roughly works up to a few MeV for the v- and w-type amplitudes. On the other hand, for the same reason given above, the applicable scaling range for the u-type amplitude is severely constrained to a lower energy ~ 1 MeV. Compared to the pionful case, all the scaling ranges here are much narrower; the reason is again that, by making the effective range of $V^{\rm PV}_{1,\rm SR}$ longer, the difference between $\langle \boldsymbol{y}_{m+} \rangle$ and $\langle \boldsymbol{y}_{m-} \rangle$ gets enhanced as the long-range part of the wave function, having a larger gradient, gets a bigger weight.

To summarize the discussions so far, we conclude that at low energy, where S-P transitions dominate, a hybrid pionful EFT analysis requires six parameters: five LECs plus $\tilde{C}^\pi_6 \propto h^1_\pi$. One may think that this conclusion makes $V^{\rm PV}_{\rm EFT}$ equivalent to $V^{\rm PV}_{\rm OME}$, which also has six PV parameters: five heavy-meson-nucleon couplings (ignoring $h^{1'}_\rho$) plus h^1_π. However, this statement is not true in general, because the six-parameter EFT framework only works under the assumption of S-P dominance, but the OME framework is not limited by this requirement. Furthermore, the OME framework implies some prescribed relationships, Eqs. (10a), (10b), (11a), and (11b), between C's and $\widetilde{C}$'s in $V^{\rm PV}_{\rm EFT}$; unfortunately, these relationships can not be justified without going to high energy. When one further restricts the analysis to very low energy, then the OPE exchange can also be absorbed and this results in a pionless version, in which only five LECs are needed.

At last, we come to the determination of the Danilov parameters, $\lambda_s^{pp,nn,np}$, λ_t, and ρ_t, which will serve as the five independent LECs. The relations between Danilov parameters and the zero-energy S-P amplitudes are given by

$$v^{NN'}(0) = -a_s^{NN'} e^{i(\delta^{NN'}_{^3P0}(0)+\delta^{NN'}_{^1S0}(0))} \lambda_s^{NN'}, \tag{24a}$$

$$u(0) = -a_t e^{i(\delta_{^1P1}(0)+\delta_{^3S1}(0))} \lambda_t, \tag{24b}$$

$$w_{\rm SR}(0) = -a_t e^{i(\delta_{^3P1}(0)+\delta_{^3S1}(0))} \rho_t, \tag{24c}$$

where a denotes the corresponding scattering length and $\delta(0)$ the zero-energy phase shift (including the Coulomb contribution) [10]. The notation "$w_{\rm SR}$" means the OPE-subtracted $^3S_1$-$^3P_1$ amplitude for the pionful theory and the full amplitude for the pionless theory (since everything is short-ranged). Using the values $a_s^{pp} = -7.8064$ fm, $a_s^{nn} = -18.487$ fm, $a_s^{np} = -23.7318$ fm, and $a_t = 5.4192$ fm, we get the dimensionless Danilov parameters

$$m_N \lambda_s^{pp} = 5.507 \times 10^{-3} \left(\tilde{D}_v^{pp} + 0.789 D_v^{pp} - 1.655\, \tilde{C}_2^{2\pi} \right), \tag{25a}$$

$$m_N \lambda_s^{nn} = 5.796 \times 10^{-3} \left(\tilde{D}_v^{nn} + 0.792 D_v^{nn} + 1.648\, \tilde{C}_2^{2\pi} \right), \tag{25b}$$

$$m_N \lambda_s^{np} = 5.778 \times 10^{-3} \left(\tilde{D}_v^{np} + 0.809 D_v^{np} \right), \tag{25c}$$

$$m_N \lambda_t = -1.462 \times 10^{-3} (\tilde{D}_u - 2.230 D_u), \tag{25d}$$

$$m_N \rho_t = 3.108 \times 10^{-3} \left(\tilde{D}_w + 0.604 D_w - 1.771\, \tilde{C}_6^{2\pi} \right), \tag{25e}$$

for the "bare" case;

$$m_N\lambda_s^{pp'} = 3.628\times10^{-3}\big(\tilde{D}_v^{pp'} + 0.849 D_v^{pp'} - 1.260\tilde{C}_2^{2\pi'}\big), \tag{26a}$$

$$m_N\lambda_s^{nn'} = 3.809\times10^{-3}\big(\tilde{D}_v^{nn'} + 0.853 D_v^{nn'} + 1.237\tilde{C}_2^{2\pi'}\big), \tag{26b}$$

$$m_N\lambda_s^{np'} = 3.772\times10^{-3}\big(\tilde{D}_v^{np'} + 0.871 D_v^{np'}\big), \tag{26c}$$

$$m_N\lambda_t' = -0.867\times10^{-3}(\tilde{D}_u' - 2.425 D_u'), \tag{26d}$$

$$m_N\rho_t' = 2.003\times10^{-3}\big(\tilde{D}_w' + 0.664 D_w' - 1.586\tilde{C}_6^{2\pi'}\big), \tag{26e}$$

for the "mod" case, and

$$m_N\lambda_s^{pp''} = 7.576\times10^{-3}\big(\tilde{D}_v^{pp''} + 1.314 D_v^{pp''}\big), \tag{27a}$$

$$m_N\lambda_s^{nn''} = 7.374\times10^{-3}\big(\tilde{D}_v^{nn''} + 1.372 D_v^{nn''}\big), \tag{27b}$$

$$m_N\lambda_s^{np''} = 7.126\times10^{-3}\big(\tilde{D}_v^{np''} + 1.396 D_v^{np''}\big), \tag{27c}$$

$$m_N\lambda_t'' = -1.053\times10^{-3}(\tilde{D}_u'' - 4.639 D_u''), \tag{27d}$$

$$m_N\rho_t'' = 2.505\times10^{-3}(\tilde{D}_w'' + 1.665 D_w''), \tag{27e}$$

for the "π-less" case. As these three calculations involve different Yukawa mass m and/or cutoff Λ_m, we use the unprimed, primed, and double-primed notations to remark the different regulator choices. However, the values of Danilov parameters, as physical quantities, should be regulator independent.

IV. PARITY-VIOLATING OBSERVABLES IN TWO-NUCLEON SYSTEMS

Having determined a minimal set of PV parameters, i.e., $m_N\lambda_s^{pp,nn,np}$, $m_N\lambda_t$, $m_N\rho_t$ and $\tilde{C}_6^{\pi}$, to describe the low-energy PV phenomena, we will use them in this section to express the PV observables which have been or will be measured in two-body systems. As analyses of these observables have been quite extensively discussed in the $V_{\rm OME}^{\rm PV}$ framework, we refer most of the details which also apply to the EFT framework to literature and only highlight the new results and the comparison with the old framework.

A. $A_L^{\vec{p}p}$ in $\vec{p}p$ scattering

The "nuclear" total asymmetry for $\vec{p}p$ scattering [21,27–31],

$$A_L^{\vec{p}p}(E) = \frac{\mathrm{Im}\left[\widetilde{\mathcal{M}}_{10,00}(E,0) + \widetilde{\mathcal{M}}_{00,10}(E,0)\right]}{\mathrm{Im}\left[\sum_{S,M_S}\mathcal{M}_{SM_S,SM_s}(E,0)\right]}, \tag{28}$$

is defined through the Coulomb-subtracted, forward ($\theta = 0$) scattering amplitude $\mathcal{M}(E,0)$, where the subscript pair $S'M_S'$, SM_S denotes the final and initial two-body spin states, respectively. As the Coulomb scattering amplitude, $M^{\rm C}$, diverges at the forward angle, the total asymmetry (with full 4π angular coverage) can only be well-defined after this singular piece is subtracted: $\mathcal{M} \equiv M - M^{\rm C}$. One should note that A_L^{pp} is not a quantity an experiment directly measures; a theoretical correction is needed to fold an experimental result into $A_L^{\vec{p}p}(E)$ (see, e.g., Refs. [21,31] for more discussions).

Currently, there are two low-energy data points at 13.6 MeV and 45 MeV which give $A_L^{\vec{p}p} = -(0.93\pm0.21)\times10^{-7}$ [4,32] and $-(1.57\pm0.23)\times10^{-7}$ [33], respectively. These supersede the earlier, less accurate experiments at 15 and 45 MeV which yield $-(1.7\pm0.8)\times10^{-7}$ [34,35] and $-(2.31\pm0.89)\times10^{-7}$ [36,37], respectively. At higher energy, there is one measurement at 221 MeV, yielding $+(0.84\pm0.29)\times10^{-7}$ [38,39]; it is motivated by the theoretical prediction that this would uniquely determine the PV ρ-exchange coupling constant $h_\rho^{pp} \equiv h_\rho^0 + h_\rho^1 + h_\rho^2/\sqrt{6}$ in $V_{\rm OME}^{\rm PV}$ [29].

The EFT analysis of $A_L^{\vec{p}p}$ for the low-energy data points is tabulated in Table III. Apparently, the observables are dominated by the S-P transition. Using the Danilov parameters obtained in the last section, we find that

$$\begin{aligned} A_L^{\vec{p}p}(13.6\ \mathrm{MeV}) &= -0.449\, m_N\lambda_s^{pp} + (-0.035 D_v^{pp} - 0.088\,\tilde{C}_2^{2\pi})\times10^{-3}, && \text{(bare)}\\ &= -0.445\, m_N\lambda_s^{pp'} + (-0.032 D_v^{pp'} - 0.157\,\tilde{C}_2^{2\pi'})\times10^{-3}, && \text{(mod)}\\ &= -0.278\, m_N\lambda_s^{pp''} + (-1.016 D_v^{pp''})\times10^{-3}; && (\pi\text{-less}) \end{aligned} \tag{29}$$

$$\begin{aligned} A_L^{\vec{p}p}(45\ \mathrm{MeV}) &= -0.795\, m_N\lambda_s^{pp} + (-0.329 D_v^{pp} - 0.395\,\tilde{C}_2^{2\pi})\times10^{-3}, && \text{(bare)}\\ &= -0.771\, m_N\lambda_s^{pp'} + (-0.276 D_v^{pp'} - 0.813\,\tilde{C}_2^{2\pi'})\times10^{-3}, && \text{(mod)}\\ &= -0.289\, m_N\lambda_s^{pp''} + (-3.207 D_v^{pp''})\times10^{-3}. && (\pi\text{-less}) \end{aligned} \tag{30}$$

In the pionful framework, the correction terms, enclosed in parentheses, are in general quite small except for the TPE part in the "mod" calculation for the 45 MeV case, which amounts to $\sim -25\%$—though somewhat larger than $\pm10\%$, but still consistent with the typical EFT expansion parameters $\sim \pm(20$–$30)\%$. Therefore, we conclude that these two data only depend on one single parameter, $m_N\lambda_s^{pp}$. In fact, the theoretical prediction for the ratio of $A_L^{\vec{p}p}(45\ \mathrm{MeV})/A_L^{\vec{p}p}(13.6\ \mathrm{MeV}) \approx -0.795/-0.449 = 1.77$ (or $-0.771/-0.445 = 1.73$ for the "mod" case) agrees very well with the experimental result $\approx -1.57/-0.93 = 1.69$ (discarding errors). Furthermore, one can see from the comparison between the "bare" and

TABLE III. Analysis of $A_L^{\vec{p}p}$ decomposed in partial waves. Each entry denotes the multiplicative coefficient for the corresponding PV coupling constant. The full result is the sum of every "entry×coupling" in the same row. The last column "OME-m" shows the numerical value of $A_L^{\vec{p}p}$ by performing the OME-mapping to the pionful EFT result with the PC and PV parameters specified in Tables I and II.

		$^1S_0-{}^3P_0(\times10^{-3})$			$^1D_2-{}^3P_2(\times10^{-3})$			$^1D_2-{}^3F_2(\times10^{-3})$			OME-m
		D_v^{pp}	$\tilde{D}_v^{pp}$	$\tilde{C}_2^{2\pi}$	D_v^{pp}	$\tilde{D}_v^{pp}$	$\tilde{C}_2^{2\pi}$	D_v^{pp}	$\tilde{D}_v^{pp}$	$\tilde{C}_2^{2\pi}$	$(\times10^{-7})$
13.6	bare	−1.980	−2.476	4.010	−0.005	0.006	−0.012	0.001	−0.001	0.002	−0.971
	mod	−1.398	−1.617	1.885	−0.004	0.004	−0.010	0.000	−0.001	0.001	−0.960
	π-less	−3.706	−2.133		−0.061	0.047		−0.012	−0.016		
45	bare	−3.686	−4.476	7.026	−0.122	0.132	−0.243	0.027	−0.033	0.064	−1.746
	mod	−2.582	−2.868	2.842	−0.089	0.094	−0.180	0.019	−0.023	0.050	−1.662
	π-less	−5.505	−2.426		−0.594	0.374		−0.155	−0.009		
221	bare	−0.069	−0.073	0.112	−2.749	2.618	−3.784	0.164	−0.388	0.633	0.426
	mod	−0.046	−0.043	0.015	−1.888	1.678	−1.636	0.086	−0.270	0.420	0.853
	π-less	−0.067	−0.018		−3.304	1.259		−0.780	−0.418		

"mod" results that even though $m_N\lambda_s^{pp}$ and $m_N\lambda_s^{pp'}$ are defined with different regulators, the expressions for $A_L^{\vec{p}p}$ in terms of them are almost regulator-independent. This justifies the advantage of using the Danilov parameters instead of the LECs C's, $\tilde{C}'s$, etc. On the other hand, one sees that the pionless analysis is not successful: not only the corrections are large, but also the theoretical prediction for $A_L^{\vec{p}p}(45\text{ MeV})/A_L^{\vec{p}p}(13.6\text{ MeV}) \approx 1.04$ is very inconsistent with the experimental result. However, this is not unexpected. These energies are higher than the upper limit (∼few MeV) under which the pionless framework is supposed to work. Therefore, in the pionless analyses, these data points should not be taken into account.

Even though it is doubtful that the $V_{\rm EFT}^{\rm PV}$ of order $O(Q)$ is sufficient for analyzing the high-energy datum at 221 MeV, it is nonetheless interesting to see how the analysis turns out to be. The result, also shown in Table III, clearly indicates the insufficiency of our S-P analysis based on the Danilov parameters. The D-P amplitude becomes the most dominant contribution, with the D-F one also being non-negligible. Both amplitudes have their own scaling factors between D_v^{pp}, $\tilde{D}_v^{pp}$, and $\tilde{C}_2^{2\pi}$ components different from the S-P amplitude. While it is not clear if the D-P and D-F amplitudes can be completely specified by D_v^{pp}, $\tilde{D}_v^{pp}$, and $\tilde{C}_2^{2\pi}$, they certainly can not be uniquely fixed by the only high-energy measurement.

By OME-mapping the EFT results in Table III, our calculations are checked with literature. The "bare+DDH-best" results are consistent with works such as Refs. [27–30], given that different strong potential models are used. The "mod+DDH-adj." results agree well with Refs. [21,31]; the small difference is because we do not use a different mass and a cutoff factor for the ω meson.

It is worth to point out that the analysis by Carlson *et al.* [21], which is based on a OME framework with two independent parameters h_ρ^{pp} and h_ω^{pp}, claims a good fit to both low- and high-energy data. Unfortunately, due to the lack of more high energy data, it is currently impossible to verify this fit along with its important dynamical assumptions—the monopole form factors and big isovector tensor coupling χ_ρ—within the EFT framework. On the other hand, their fitted PV ωNN coupling constant, $h_\omega^{pp} = h_\omega^0 + h_\omega^1$, is only marginally consistent with most hadronic predictions and needs further clarification. For these issues, we refer to Ref. [40] for more discussions.

Finally, we turn our attention to the MR contributions, which have not received extensive study and are left out while we do the OME-mapping in Table III. By writing out $\tilde{C}_2^{2\pi}$ in term of h_π^1 explicitly and assuming the DDH best value for h_π^1, one sees the asymmetry in the "bare" case increased by ∼70% for the 13.6 and 45 MeV data points and ∼60% for the 221 MeV one. In the "mod" case, the increases are ∼30% and ∼20% for low- and high-energy cases, respectively. Since $V_{1,\rm MR}^{\rm PV}$ and $V_{1,\rm SR}^{\rm PV}$ have the same power counting, it is not unnatural to expect their contributions have similar magnitude. Another remark concerns the general trends that the TPE enhances the asymmetry and it is the the low-energy cases that get more boost than the high-energy ones. These points have also been noticed in Ref. [40], where part of the TPE contribution is accounted for by formulating it as a ρ-resonance.

B. $\phi_n^{\vec{n}p}$ and P_n^{np} in neutron transmission through parahydrogen

It was first pointed by Michel [41] and later on by Stodolsky [42,43] that nuclear parity violation can be studied through low-energy neutron transmission, where the whole process acts like optics. The observables could be a spin rotation, ϕ_n, about the longitudinal axis (assumed to be $\hat{z}$) for the transversely-polarized neutron, or a net longitudinal polarization, P_n, that an unpolarized neutron beam picks up when traversing through medium—the latter is equivalent to the asymmetry in cross section for the longitudinally-polarized neutron scattering, $A_L^{\vec{n}p}$. These quantities per unit length (assuming the target is uniform), $d\phi_n/dz$ and dP_n/dz, can be related to the PV forward scattering amplitude $\tilde{M}(E,0)$ by

$$\frac{d\phi_n}{dz} = -\frac{2\pi}{k} N \mathrm{Re}(\tilde{M}_{+z}(E,0) - \tilde{M}_{-z}(E,0)), \qquad (31)$$

$$\frac{dP_n}{dz} = -\frac{2\pi}{k} N \mathrm{Im}(\tilde{M}_{+z}(E,0) - \tilde{M}_{-z}(E,0)), \qquad (32)$$

TABLE IV. Analysis of (I) $d\phi_n^{\vec{n}p}(\text{th.})/dz$ in rad/m and (II) $dP_n^{np}(\text{th.})/dz$ in 10^{-4}/m decomposed in partial waves. See Table III for the explanation of tabularization.

		$^1S_0-{}^3P_0(\times10^{-2})$		$^3S_1-{}^1P_1(\times10^{-2})$		$^3S_1-{}^3P_1(\times10^{-2})$				OME-m ($\times10^{-7}$)
		D_v^{np}	$\tilde{D}_v^{np}$	D_u	$\tilde{D}_u$	D_w	$\tilde{D}_w$	$\tilde{C}_6^{\pi}$	$\tilde{C}_6^{2\pi}$	
(I)	bare	1.169	1.444	−0.186	0.083	0.214	0.355	0.286	−0.628	6.711
	mod	0.821	0.943	−0.120	0.049	0.152	0.229	0.284	−0.363	5.149
	π-less	2.487	1.781	−0.279	0.060	0.476	0.286			
(II)	bare	4.805	5.939	0.175	−0.079	−0.202	−0.334	−0.269	0.591	2.165
	mod	3.378	3.878	0.113	−0.047	−0.143	−0.215	−0.267	0.341	−2.220
	π-less	10.227	7.325	0.262	−0.057	−0.269	−0.448			

where k is the magnitude of the neutron momentum, N is the target number density, and the subscript $\pm z$ denotes the direction of neutron polarization.

For a thermal neutron beam, $E_n \approx 0.025$eV, transmitting through liquid parahydrogen, $N = 0.24 \times 10^{23}/\text{cm}^3$, the EFT analysis of $d\phi_n/dz$ and dP_n/dz is tabulated in Table IV. At thermal energy, the magnitude of dP_n^{np}/dz is about four orders of magnitude smaller than $d\phi_n^{\vec{n}p}/dz$. When neutron energy is further decreased, $d\phi_n^{\vec{n}p}/dz$ stays constant, but dP_n^{np}/dz drops as $\sqrt{E_n}$; therefore, the spin-rotation measurement is more feasible for low-energy neutrons. This trend is consistent with the argument made by Stodolsky [43] about the elastic scattering. It is also pointed out in Ref. [43] that exothermic processes, i.e., inelastic exit channels, can possibly result in a nonvanishing dP_n/dz at zero energy. However, it is not the case for np scattering, where the only exothermic reaction, $np \to d\gamma$ (will be discussed in Sec. IV D), does not lead to a total asymmetry, as remarked in Ref. [44].

In this case, all three different S-P amplitudes come into play, and the results in terms of Danilov parameters and $\tilde{C}_6^{\pi}$ (in pionful theory) are

$$\left.\frac{d\phi_n^{\vec{n}p}(\text{th.})}{dz}\right|_{\text{m/rad}} \begin{aligned} &= 2.500\, m_N \lambda_s^{np} - 0.571\, m_N \lambda_t + 1.412\, m_N \rho_t + 0.286\, \tilde{C}_6^{\pi} + (0.000), && \text{(bare)} \\ &= 2.500\, m_N \lambda_s^{np'} - 0.571\, m_N \lambda_t' + 1.412\, m_N \rho_t' + 0.284\, \tilde{C}_6^{\pi} + (0.000), && \text{(mod)} \\ &= 2.500\, m_N \lambda_s^{np''} - 0.571\, m_N \lambda_t'' + 1.412\, m_N \rho_t'' + (0.000). && (\pi\text{-less}) \end{aligned} \tag{33}$$

Because this process is close to zero energy, it is not a surprise that the Danilov parameters work extremely well (almost no error). The result does not depend on the Yukawa mass m and cutoff Λ_m. Furthermore, the OPE contribution can be effectively included in the pionless framework as the last line shows. Therefore, these two EFT analyses are very consistent in this case.

By OME-mapping the EFT results, the "bare+DDH-best" value, $d\phi_n^{\vec{n}p}(\text{th.})/dz \simeq 6.71 \times 10^{-7}$ rad/m, is about 20% smaller in magnitude than an early prediction using the Paris potential [45], and with a different sign. Thus, we confirm the assertion of Ref. [22] about the sign problem in Ref. [45]. As for the "mod+DDH-adj" value, $\simeq 5.15 \times 10^{-7}$ rad/m, it agrees well with Ref. [22]. If these numerical estimates are not too far off, the plan of doing such an experiment aiming at a 2.7×10^{-7} rad/m precision [46] at the Spallation Neutron Source (SNS) will certainly provide a valuable data point.

The MR contribution enters through the $^3S_1$–$^3P_1$ transition. Because $\tilde{C}_6^{\pi}$ and $\tilde{C}_6^{2\pi}$ have the same sign, Table IV suggests that the MR term reduces the OPE contribution which dominates the above OME-m estimates. The correction is about −15% for the "bare" calculation, and −10% for the "mod" calculation. This ∼10% correction is consistent with the qualitative power-counting argument that the MR contribution is smaller than the leading OPE one by an order of magnitude.

C. P_γ^{np} in $np \to d\gamma$ and $A_L^{\vec{\gamma}d}$ in $\vec{\gamma}d \to np$

Low-energy radiative neutron capture mainly involves the lowest-order electromagnetic transitions. For $np \to d\gamma$, it is $M1$ for the PC part, and $E1$ for the PV part. Since the total cross section is dominated by the $^1S_0$-wave scattering, the nonzero circular polarization takes an approximate simple form as

$$P_\gamma^{np} = 2\frac{\langle \mathcal{D}||E_1||\widetilde{^3P_0}\rangle + _{\mathcal{D}}\langle \widetilde{^1P_1}||E_1||^1S_0\rangle}{\langle \mathcal{D}||M_1||^1S_0\rangle}, \tag{34}$$

where the double bar "||" denotes the reduced matrix element. In this case, the observable depends on the $^1S_0$-$^3P_0$ and the deuteron $\mathcal{D}$-$^1P_1$ admixtures. It is important to recognize that we rely on the Siegert theorem [47], through which the E_1 operator is related to the charge dipole operator C_1, to calculate the $E1$ matrix elements. This manipulation not only

TABLE V. Analysis of P_γ^{np}(th.) decomposed in partial waves. See Table III for the explanation of tabularization.

	$^1S_0 - {}^3P_0$ mix.	$(\times 10^{-3})$	$\mathcal{D} - {}^1P_1$ mix.	$(\times 10^{-3})$	OME-m $(\times 10^{-7})$
	D_v^{np}	$\tilde{D}_v^{np}$	D_u	$\tilde{D}_u$	
bare	−0.751	−0.935	2.166	−0.980	0.247
mono	−0.525	−0.607	1.391	−0.580	0.520
π-less	−1.367	−0.981	3.156	−0.972	

implicitly includes most $\mathcal{O}(v/c)$ meson exchange currents, but also imposes a $\Delta S = 0$ spin selection rule as shown in Eq. (34).

For thermal neutron, the EFT analysis is tabulated in Table V. In terms of Danilov parameters, the result can be expressed as

$$\begin{aligned} P_\gamma^{np}(\text{th.}) &= -0.161\, m_N \lambda_s^{np} + 0.670\, m_N \lambda_t + (0.005 D_v^{np} + 0.019 D_u) \times 10^{-3}, \quad \text{(bare)} \\ &= -0.161\, m_N \lambda_s^{np'} + 0.669\, m_N \lambda_t' + (0.004 D_v^{np'} + 0.016 D_u') \times 10^{-3}, \quad \text{(mod)} \\ &= -0.138\, m_N \lambda_s^{np''} + 0.923\, m_N \lambda_t'' + (0.002 D_v^{np'} + 1.361 D_u'') \times 10^{-3}. \quad (\pi\text{-less}) \end{aligned} \tag{35}$$

Although the observable P_γ^{np} is not determined directly by the scattering amplitudes—as shown in Eq. (34), it involves parity admixtures and transition matrix elements—the Danilov parameters still do a good job in the pionful analyses. However, this is not the case for the pionless case. In particular for the $\mathcal{D}$-$^1P_1$ part (u-type amplitude), the correction term is too big to make the analysis reliable. As one can see from the central bottom panel of Fig. 5, the scaling of u^+ and u^- amplitudes already poses a serious problem not far from threshold; the deuteron binding energy, though small, could be worrisome already. Therefore, we shall rely on the pionful analysis for this observable, and leave the inconsistency with pionless theory for future study.

The OME-mapping gives the "bare+DDH-best" value $P_\gamma^{np}(\text{th.}) = 2.5 \times 10^{-8}$ which agrees well with a recent calculation [48] and is also consistent with pre-80's predictions, e.g., Refs. [8,49–52], around $(2–5) \times 10^{-8}$, (see Ref. [53] for a summary). For the "mod+DDH-adj." value $P_\gamma^{np}(\text{th.}) = 0.52 \times 10^{-7}$, we have an excellent check with Ref. [22].

Historically, the first measurement of P_γ^{np}(th.) done by the Leningrad group reports a result $-(1.3 \pm 0.45) \times 10^{-6}$ [54], which not only exceeds most theoretical predictions by two orders of magnitude but also has an opposite sign. The follow-up experiment does correct the sign problem; however, the published result $P_\gamma^{np}(\text{th.}) = (1.8 \pm 1.8) \times 10^{-7}$ [55] still has too large an error bar. In order to circumvent the difficulty of measuring a circular polarization, the inverse process, the asymmetry $A_L^{\vec{\gamma}d}$ in deuteron photo-disintegration, $\vec{\gamma}d \to np$, can be a good alternative. By detailed balancing, $A_L^{\vec{\gamma}d} = P_\gamma^{np}$ if all kinematics are exactly reversed. One can show that, for photon with energy of 1.32 keV above the threshold, $A_\gamma^{\vec{\gamma}d}(1.32\ \text{keV}+) = P_\gamma^{np}(\text{th.})$.

As demonstrated in several theoretical works [22,56–59], the asymmetry $A_L^{\vec{\gamma}d}$ gets larger when approaching the threshold, but on the other hand, the total cross section gets smaller. There are two data points reported in 80s: $(2.7 \pm 2.8) \times 10^{-6}$ at $E_\gamma = 4.1$ MeV and $(7.7 \pm 5.3) \times 10^{-6}$ at $E_\gamma = 3.2$ MeV [60,61]; though they qualitatively justify the statement above, the precisions are too low to be of use. As indicated in Ref. [18], there seem to be several group showing interests of such new measurements.

An important point to note for this particular observable analyzed in the OME framework is that, unlike the case for neutron transmission, the $\mathcal{D}$-$^1P_1$ admixture has an important contribution so that the model dependence is worrisome. The situation is most clear when comparing with other semi- and nonlocal potential model calculations. As shown in Refs. [22,48], the CD-Bonn and Bonn-B calculations give predictions two times larger, and the Bonn calculation even enhances by an order of magnitude. The difference is mostly due to the large variations of these models in the $^1P_1$ channel at short distances [48]. However, in the EFT treatment, this model-dependence can be absorbed in the Danilov parameters and all that matters is the result in Eq. (35).

D. A_γ in $\vec{n}p \to d\gamma$

By the same approximation as in the above subsection, the photon asymmetry in $\vec{n}p \to d\gamma$, $A_\gamma^{\vec{n}p}$, which is defined through $d\sigma_\pm(\theta)/d\Omega \propto 1 \pm A_\gamma^{\vec{n}p} \cos\theta$,[8] can be expressed as

$$A_\gamma^{\vec{n}p} = -\sqrt{2}\frac{\langle \mathcal{D}||E_1||\widetilde{^3P_1}\rangle + {}_{\mathcal{D}}\langle \widetilde{^3P_1}||E_1||^3S_1\rangle}{\langle \mathcal{D}||M_1||^1S_0\rangle}. \tag{36}$$

[8]From this expression, one clearly sees $\int d\Omega d\sigma_+(\theta) = \int d\Omega d\sigma_-(\theta)$. This confirms the earlier statement that $A_L^{\vec{n}p}$ vanishes at zero energy, even if an exothermic process exists.

TABLE VI. Analysis of $A_\gamma^{\vec{n}p}$(th.) decomposed in partial waves. See Table III for the explanation of tabularization.

	$^3S_1 - {}^3P_1$ mix. ($\times 10^{-3}$)				$\mathcal{D}$–$^3P_1$ mix. ($\times 10^{-3}$)				OME-m ($\times 10^{-7}$)
	D_w	$\tilde{D}_w$	$\tilde{C}_6^\pi$	$\tilde{C}_6^{2\pi}$	D_w	$\tilde{D}_w$	$\tilde{C}_6^\pi$	$\tilde{C}_6^{2\pi}$	
bare	−0.108	−0.185	−0.133	0.321	−0.066	−0.103	−0.139	0.193	−0.506
mod	−0.076	−0.118	−0.132	0.172	−0.048	−0.069	−0.138	0.128	−0.486
π-less	−0.197	−0.133			−0.212	−0.139			

Unlike the case for P_γ^{np}, it is the $^3S_1$-$^3P_1$ and $\mathcal{D}$–$^3P_1$ admixtures that contribute in this case.

For thermal neutron, the EFT analysis is tabulated in Table VI, and expressed as

$$\begin{aligned} A_\gamma^{\vec{n}p}(\text{th.}) &= -0.093\, m_N \rho_t - 0.272\, \tilde{C}_6^\pi + \left(0.003\, \tilde{C}_6^{2\pi}\right) \times 10^{-3}, \quad \text{(bare)} \\ &= -0.093\, m_N \rho_t' - 0.270\, \tilde{C}_6^{\pi'} + \left(0.004\, \tilde{C}_6^{2\pi'}\right) \times 10^{-3}, \quad \text{(mod)} \\ &= -0.109\, m_N \rho_t'' + (0.044 D_w'') 10^{-3}. \quad (\pi\text{-less}) \end{aligned} \tag{37}$$

Again, the Danilov parameter $m_N \rho_t$ pretty much summarizes the short-distance physics in the pionful analyses, and the result is independent of the regulators. Comparatively, the pionless analysis has a much larger correction term which is about 10%. Given this error bar, the pionless analysis can be considered being consistent with the pionful analysis, and again we leave the resolution for this small error for future study.

The OME-mapping values, $A_\gamma^{\vec{n}p}(\text{th.}) = -5.06 \times 10^{-8}$ for the "bare+DDH-best" case and -4.85×10^{-8} for the "bare+DDH-adj." case, are consistent with existing predictions, e.g., Refs. [8,48,49,51,53,62–65] for the former and Refs. [22,66] for the latter, respectively.

The MR contributions change the above OME-m results somewhat. Their corrections to the OPE contributions are −13% and −8% for the "bare" and "mod" cases, respectively. This is similar to the neutron spin rotation case, and consistent with a recent calculation [24].

The great interest of measuring $A_\gamma^{\vec{n}p}$ is mainly because it is dominated by the OPE in the $V_{\text{OME}}^{\text{PV}}$ framework. This can also be observed from the above EFT analysis: If one assumes the natural size of $m_N \rho_t / \tilde{C}_6^\pi \sim 0.1$, the OPE contribution then dominates the SR one by a factor of 30 or so.[9] One of the outstanding puzzles in nuclear PV is the difficulty of accommodating the extremely small upper limit on h_π^1, set by the ^{18}F results [3], with hadronic predictions and other nuclear PV experiments. The NPDGamma experiment [67], currently running at the Los Alamos Neutron Science Center (LANSCE) and will be at SNS later on, aims to reach an ultimate sensitivity of 5×10^{-9}. Results from this experiment will certainly improve the long-existing value: $(0.6 \pm 2.1) \times 10^{-7}$ [61,68], and hopefully resolve the h_π^1 puzzle.

Concluding this section, we shall make an important remark about the PV meson exchange current (MEC) effects which manifest in electromagnetic processes such as radiative neutron capture being discussed here and in Sec. IV C. Although the Siegert theorem alleviates much of the problem regarding the calculations of transverse electric multipole operators E_J's due to MECs, there is no easy simplification when the transverse magnetic multipole operators M_J's are concerned. Furthermore, the Siegert theorem only applies to MECs which are constrained by the continuity equation; for other transverse MECs, their effects to E_J's have to be added separately.

In Ref. [18], there is indeed such a transverse MEC, which can not be accounted for by gauging the PV interaction, and it introduces a new PV constant designated as $\bar{c}_\pi$. This MEC takes the following form in the configuration space:

$$\begin{aligned} &\boldsymbol{j}_{\bar{c}_\pi}(\boldsymbol{x}; \boldsymbol{x}_1, \boldsymbol{x}_2) \\ &\quad = -i \frac{\sqrt{2} g_\pi \bar{c}_\pi}{m_N \Lambda_\chi F_\pi} (\tau_{1+}\tau_{2-})[\boldsymbol{\sigma}_2 \cdot \hat{r} \boldsymbol{\sigma}_1 \times \boldsymbol{\nabla}_x \delta^{(3)}(\boldsymbol{x} - \boldsymbol{x}_1)] \\ &\qquad \times \frac{e^{-m_\pi r}}{4\pi r^2}(1 + m_\pi r) + (1 \leftrightarrow 2), \end{aligned} \tag{38}$$

where $\tau_\pm = \tau_x \pm i\tau_y$, and $r = |\boldsymbol{x}_1 - \boldsymbol{x}_2|$. Compared with the dominant part of the PV OPE MEC, the so-called pair current (which is constrained by the Siegert theorem, so its contribution has already been implicitly

[9] We stress that this argument is based on naturalness. Without further experimental confirmation, one should still keep other possibilities open.

calculated),

$$\begin{aligned}\boldsymbol{j}_{\pi\mathrm{pair}}(\boldsymbol{x};\boldsymbol{x}_1,\boldsymbol{x}_2) &= -\frac{g_\pi h_\pi^1}{2\sqrt{2}m_N}\left(\boldsymbol{\tau}_1\cdot\boldsymbol{\tau}_2-\tau_1^z\tau_2^z\right)[\boldsymbol{\sigma}_1\delta^{(3)}(\boldsymbol{x}-\boldsymbol{x}_1)] \\ &\quad\times\frac{\mathrm{e}^{-m_\pi r}}{4\pi r}+(1\leftrightarrow 2),\end{aligned} \tag{39}$$

the matrix element $\langle \boldsymbol{j}_{\bar{c}_\pi}\rangle$ roughly scales with $\langle \boldsymbol{j}_{\pi\mathrm{pair}}\rangle$ by a factor $\langle -i\boldsymbol{\nabla}_x/\Lambda_\chi\rangle = k/\Lambda_\chi$, assuming $\langle r\rangle \sim 1/m_\pi$ for typical nuclei. Therefore, for the radiative processes considered in this work, where the photon energy k is just a few MeV so that $k/\Lambda_\chi \lesssim 1\%$, the contribution of $\boldsymbol{j}_{\bar{c}_\pi}$ is negligible. Hence we do not have to include this extra PV constant $\bar{c}_\pi$ in the current search program at low energy.

V. SUMMARY

In this work, we study the newly-proposed search program for nuclear parity violation based on the effective field theory framework [18]. It is found that, in a hybrid EFT treatment, the nuclear PV phenomena at low energy, where S-P transitions dominate, can be well specified by six parameters. These six parameters to be determined phenomenologically are the five dimensionless Danilov parameters: $m_N\lambda_s^{pp,nn,np}$, $m_N\lambda_t$ and $m_N\rho_t$, and the long-range one-pion-exchange parameter $\tilde{C}_6^\pi$, which is proportional to the parity-violating pion-nucleon coupling constant h_π^1.

The two-body parity-violating observables being studied in this work are summarized as following:

$$A_L^{\vec{p}p}(13.6\,\mathrm{MeV}) = -0.45 m_N\lambda_s^{pp}, \tag{40}$$

$$A_L^{\vec{p}p}(45\,\mathrm{MeV}) = -0.78 m_N\lambda_s^{pp}, \tag{41}$$

$$\begin{aligned}\frac{d}{dz}\phi_n^{\vec{n}p}(\mathrm{th.})|_{\mathrm{rad/m}} &= 2.50\, m_N\lambda_s^{np} - 0.57\, m_N\lambda_t \\ &\quad + 1.41\, m_N\rho_t + 0.29\,\tilde{C}_6^\pi,\end{aligned} \tag{42}$$

$$\begin{aligned}P_\gamma^{np}(\mathrm{th.}) &= -0.16\, m_N\lambda_s^{np} + 0.67\, m_N\lambda_t \\ &= A_L^{\vec{\gamma}d}(1.32\,\mathrm{keV}+),\end{aligned} \tag{43}$$

$$A_\gamma^{\vec{n}p}(\mathrm{th.}) = -0.093\, m_N\rho_t - 0.27\,\tilde{C}_6^\pi. \tag{44}$$

Because $A_L^{\vec{p}p}(13.6\,\mathrm{MeV})$ and $A_L^{\vec{p}p}(45\,\mathrm{MeV})$ essentially determine the same quantity, $m_N\lambda_s^{pp}$, these equations only serve as four constraints—if precise data can all be obtained for the three listed neutron experiments. In order to have at least two more linearly-independent equations, other experimental possibilities have to be explored. In few-body systems, where reliable theoretical analyses can be performed, the candidate reactions include $pd, nd, p\alpha, n\alpha$, etc.—just to name a few. Currently, there are a published datum for $p\alpha$: $A_L^{\vec{p}\alpha}(45\,\mathrm{MeV}) = -(3.3\pm 0.9)\times 10^{-7}$ [69], and an ongoing experiment of thermal neutron spin rotation in liquid helium, $\phi_n^{\vec{n}\alpha}(th.)$, at the National Institute of Standard and Technology [46]. In this respect, existing calculations of these PV five-body processes should be updated. Because alpha particle is a tightly bound state such that nucleons inside have larger momenta, whether the S-P dominance—the cornerstone of this six-parameter analysis—can still hold should be carefully examined. On the other hand, low-energy reactions involving d or t might suffer less the problem. However, in order to motivate new experiments, updated theoretical works are indispensable.

ACKNOWLEDGMENTS

The author would like to thank B. R. Holstein and M. J. Ramsey-Musolf for the encouragement of taking on this project. The useful discussions with them and J. A. Carlson, B. Desplanques, W. C. Haxton, and U. van Kolck are deeply appreciated. Part of this work was supported by the Dutch Stichting vor Fundamenteel Onderzoek der Materie (FOM) under program 48 (TRIμP) and the U.S. Department of Energy under contract DE-AC52-06NA25396.

[1] N. Tanner, Phys. Rev. **107**, 1203 (1957).
[2] V. M. Lobashov, V. A. Nazarenko, L. F. Saenko, L. M. Smotritsky, and G. I. Kharkevitch, Phys. Lett. **B25**, 104 (1967).
[3] E. G. Adelberger and W. C. Haxton, Annu. Rev. Nucl. Part. Sci. **35**, 501 (1985).
[4] W. Haeberli and B. R. Holstein, in *Symmetries and Fundamental Interactions in Nuclei*, edited by W. C. Haxton and E. M. Henley (World Scientific, Singapore, 1995), pp. 17–66.
[5] B. Desplanques, Phys. Rep. **297**, 1 (1998).
[6] M. J. Ramsey-Musolf and S. A. Page, Ann. Rev. Nucl. Part. Sci. **56**, 1 (2006).
[7] G. S. Danilov, Phys. Lett. **18**, 40 (1965).
[8] G. S. Danilov, Phys. Lett. **B35**, 579 (1971).
[9] G. S. Danilov, Sov. J. Nucl. Phys. **14**, 443 (1972).
[10] B. Desplanques and J. Missimer, Nucl. Phys. **A300**, 286 (1978).
[11] B. Desplanques and J. Missimer, Phys. Lett. **B84**, 363 (1979).
[12] R. J. Blin-Stoyle, Phys. Rev. **118**, 1605 (1960).
[13] R. J. Blin-Stoyle, Phys. Rev. **120**, 181 (1960).
[14] G. Barton, Nuovo Cimento **19**, 512 (1961).
[15] B. Desplanques, J. F. Donoghue, and B. R. Holstein, Ann. Phys. (NY) **124**, 449 (1980).
[16] W. C. Haxton, C.-P. Liu, and M. J. Ramsey-Musolf, Phys. Rev. Lett. **86**, 5247 (2001).
[17] W. C. Haxton, C.-P. Liu, and M. J. Ramsey-Musolf, Phys. Rev. C **65**, 045502 (2002).
[18] S.-L. Zhu, C. M. Maekawa, B. R. Holstein, M. J. Ramsey-Musolf, and U. van Kolck, Nucl. Phys. **A748**, 435 (2005).
[19] C.-P. Liu and M. J. Ramsey-Musolf (in preparation).
[20] R. B. Wiringa, V. G. J. Stoks, and R. Schiavilla, Phys. Rev. C **51**, 38 (1995).
[21] J. Carlson, R. Schiavilla, V. R. Brown, and B. F. Gibson, Phys. Rev. C **65**, 035502 (2002).
[22] R. Schiavilla, J. Carlson, and M. W. Paris, Phys. Rev. C **70**, 044007 (2004).
[23] C.-P. Liu, G. Prézeau, and M. J. Ramsey-Musolf, Phys. Rev. C **67**, 035501 (2003).
[24] C. H. Hyun, S. Ando, and B. Desplanques, nucl-th/0609015.

[25] R. Machleidt, Phys. Rev. C **63**, 024001 (2001).
[26] B. Desplanques, Nucl. Phys. **A335**, 147 (1980).
[27] M. Simonius, Phys. Lett. **B41**, 415 (1972).
[28] M. Simonius, Nucl. Phys. **A220**, 269 (1974).
[29] M. Simonius, Can. J. Phys. **66**, 548 (1988).
[30] F. Nessi-Tedaldi and M. Simonius, Phys. Lett. **B215**, 159 (1988).
[31] D. E. Driscoll and G. A. Miller, Phys. Rev. C **39**, 1951 (1989).
[32] P. D. Eversheim *et al*., Phys. Lett. **B256**, 11 (1991).
[33] S. Kistryn *et al*., Phys. Rev. Lett. **58**, 1616 (1987).
[34] J. M. Potter *et al*., Phys. Rev. Lett. **33**, 1307 (1974); Erratum: *ibid.* **33**, 1594 (1974).
[35] D. E. Nagle *et al*., in *High Energy Physics with Polarized Beams and Polarized Targets-1978*, AIP Conf. Proc. No. 51, edited by G. H. Thomas (AIP, New York, 1979), p. 218.
[36] R. Balzer *et al*., Phys. Rev. Lett. **44**, 699 (1980).
[37] R. Balzer *et al*., Phys. Rev. C **30**, 1409 (1984).
[38] A. R. Berdoz *et al*., Phys. Rev. Lett. **87**, 272301 (2001).
[39] A. R. Berdoz *et al*., Phys. Rev. C **68**, 034004 (2003).
[40] C. P. Liu, C. H. Hyun, and B. Desplanques, Phys. Rev. C **73**, 065501 (2006).
[41] F. C. Michel, Phys. Rev. **133**, B329 (1964).
[42] L. Stodolsky, Phys. Lett. **B50**, 352 (1974).
[43] L. Stodolsky, Nucl. Phys. **B197**, 213 (1982).
[44] C. P. Liu and R. G. E. Timmermans, Phys. Lett. **B634**, 488 (2006).
[45] Y. Avishai and P. Grange, J. Phys. G **10**, L263 (1984).
[46] D. Markov, http://www.int.washington.edu/talks/WorkShops/int_02_3/People/Markoff_D/ (2002).
[47] A. J. F. Siegert, Phys. Rev. **52**, 787 (1937).
[48] C. H. Hyun, S. J. Lee, J. Haidenbauer, and S. W. Hong, Eur. Phys. J. A **24**, 129 (2005).
[49] D. Tadic, Phys. Rev. **174**, 1694 (1968).
[50] K. R. Lassey and B. H. J. McKellar, Phys. Rev. C **11**, 349 (1975).
[51] B. Desplanques, Nucl. Phys. **A242**, 423 (1975).
[52] B. A. Craver, E. Fischbach, Y. E. Kim, and A. Tubis, Phys. Rev. D **13**, 1376 (1976); Erratum: *ibid.* **14**, 313 (1976).
[53] K. R. Lassey and B. H. J. McKellar, Nucl. Phys. **A260**, 413 (1976).
[54] V. M. Lobashov *et al*., Nucl. Phys. **A197**, 241 (1972).
[55] V. A. Knyaźkov *et al*., Nucl. Phys. **A417**, 209 (1984).
[56] H. C. Lee, Phys. Rev. Lett. **41**, 843 (1978).
[57] T. Oka, Phys. Rev. D **27**, 523 (1983).
[58] M. Fujiwara and A. I. Titov, Phys. Rev. C **69**, 065503 (2004).
[59] C. P. Liu, C. H. Hyun, and B. Desplanques, Phys. Rev. C **69**, 065502 (2004).
[60] E. D. Earle *et al*., Can. J. Phys. **66**, 534 (1988).
[61] J. Alberi *et al*., Can. J. Phys. **66**, 542 (1988).
[62] D. B. Kaplan, M. J. Savage, R. P. Springer, and M. B. Wise, Phys. Lett. **B449**, 1 (1999).
[63] M. J. Savage, Nucl. Phys. **A695**, 365 (2001).
[64] B. Desplanques, Phys. Lett. **B512**, 305 (2001).
[65] C. H. Hyun, T.-S. Park, and D.-P. Min, Phys. Lett. **B516**, 321 (2001).
[66] R. Schiavilla, J. Carlson, and M. Paris, Phys. Rev. C **67**, 032501(R) (2003).
[67] W. M. Snow *et al*., Nucl. Instrum. Methods A **440**, 729 (2000).
[68] J. F. Cavaignac, B. Vignon, and R. Wilson, Phys. Lett. **B67**, 148 (1977).
[69] J. Lang *et al*., Phys. Rev. C **34**, 1545 (1986).